

Effects of mullite gel on the properties of alumina castables

Simon Jeya Sunder Raj* and S. Manisha Vidyavathy

Department of Ceramic Technology, A.C.Tech Campus, Anna University, Chennai-600025

The bauxite-based refractory castables are made up of well-graded bauxite aggregate, binding matrix, and a sufficient amount of water. There are four mullite samples with various percentages of sol such as 2%, 5%, 7% and 10% were added to the alumina castables compositions. The conventional castables processing is carried out and after heat treatment the resultant product is characterized. Prepared castables are characterized by X-ray diffraction (XRD), Scanning Electron Microscopy (SEM) and Differential scanning calorimetry (DSC) to obtain the structural properties, morphology, and thermal analysis, respectively. Enhanced properties were obtained for the mullite samples with 5% and 7% sols. Considerably improved flexural strength, modulus of rupture (MOR) and pH levels are obtained for the mullite gel composition but with a relatively lower level of permanent linear change (PLC). Great refractory properties were achieved after sintering at 1300 °C due to the presence of mullite in the bond phase with very slight CaO. This enables their use in various refractory applications such as in steel ladles, furnaces, kilns, incinerators, and reactors.

Keywords: Mullite, Alumina, Refractory castable, Characterization, XRD, Microstructure

Introduction

Refractory castables have been widely used in the last few years. The demand for ceramic production and installation technology has occurred due to various advantages of decreasing the number of calcinations, joints, low corrosion, and so on. Bauxite-based castables have been widely used in the various paths of the blast furnace because of their excellent properties [1]. One of the important constituents of the castable making process is the binder of the castables. The purpose of the binder is to elongate the strength of the green stage at high temperatures. It decomposes the binder on heating and increases the strength of the castables formed as fine reactant particles after the heating process [2].

Usually, calcium aluminate cement is used as a hydraulic binder for bauxite-based refractories. However, the strength of the castables decreases due to the decomposition of hydration products and these form low melting phases which degrade the performances of the castables [3]. Though cement is an essential binder, due to the low melting eutectics at high temperatures, it is not used as the main binder of the refractory castables composition. To address this problem, a castable has been made using cement-free binder systems for high-temperature applications [4].

The addition of additives prepared by using the sol-gel route has become popular in the castable preparation. These additives comprise ultrafine particles of the same

composition as the castables surround the refractory materials through a polymeric network and develop a ceramic bonding during heating [5]. These compositions have better flow properties and are highly flexible during installation [6].

Cement-free bonding solutions for high-temperature applications have therefore been the focus. Colloidal silica has been used as a binder (using sol-gel-based coagulation bonding) in many studies. Due to its ease of processing and lack of need for any property-modifying additive, the sol-gel bonding technique is more beneficial than other systems. At high temperatures, ultrafine silica particles in the alumina castable system create mullite bonds, which improve the castables characteristics [7-9].

However, the presence of free silica and the development of a liquid phase above the eutectic temperature have hindered the utilization of Al₂O₃-SiO₂ combination for very high-temperature applications [5, 10, 11]. However, as the processing temperatures of the user industries increased, the demand for extremely pure high temperature performance castables also increased.

When utilised as additives, ceramic powders such as alumina, mullite, spinel, and others processed by using the sol-gel method have shown to improve alumina castables properties [12, 13]. However, there has only been a random attempt in the literature to use these ceramic systems as bonding materials in castables. Although several studies have reported using alumina (boehmite) sol as a binder [14, 15], the general application of alumina sol binders is limited because of many production challenges [12].

In some studies, mullite precursor sol has been used

*Corresponding author:
Tel : +91 9940471851
E-mail: simon16.peter@gmail.com

as a binder [16, 17]. The silica-alumina sol bonding agent was made from ethyl silicate and aluminum isopropanol using the sol-gel method.

When compared to cement-bonded formulations, the characteristics are enhanced [16]. Microstructures were linked to pore development, fracture production due to volume imbalance, and there is an excessive grain growth when mullite sol was combined with alumina cement and micro-silica.

Mullite sol, even when used in association with alumina cement, was shown to have poorer characteristics, both at ambient and higher temperatures, when compared to solely cement and silica sol bonded formulations [17]. Numerous researchers have utilised refractory cement as a supplementary binder but the use of alumina or mullite sol as a binder is yet to be explored.

Chemical precursors were employed in the wet chemical synthesis of the mullite sol, which was then tested for different characteristics. This stable mullite sol was used as a binder in a high purity alumina castable system at two different percentages [12].

The purpose of this analysis is to study about high-alumina (in mullite forming) refractory castables combined with silica and 0.1% or 0.3 wt.% MgO to trigger rapid liquid phase sintering. After heat treatment at different temperatures up to 1300 °C, mullite sol bonded compositions were processed conventionally and evaluated for various refractory characteristics. The castable produced with commercial silica sol as a bond is also compared to the developed castables.

Materials and Methods

Synthesis of precursor materials

Materials

The precursor materials were prepared using a solution of aluminum nitrate nonahydrate ($\text{AlH}_{18}\text{N}_3\text{O}_{18}$) (RFCL, New Delhi) solution as an alumina source, silicon tetraethyl orthosilicate (TEOS) $\text{Si}(\text{OC}_2\text{H}_5)_4$ (Merck, India) as silica source, and ammonia (NH_3) (Merck, India) [9, 18]. The mullite precursor was taken in the stoichiometric ratio of 2:1 (alumina and silica). The pH range of mullite gel was maintained between 2.5 and 5.

Hydrolysis condensation

Sol-gel preparation

The steps involved in the synthesis of mullite precursor sol are as follows: The mullite precursor was prepared at room temperature. The solution was set aside and stirred continuously using a magnetic stirrer for 15-20 min to obtain homogenization. The alumina nitrate solution was added drop wise to the TEOS solution and was continuously stirred for 60 to 90 min. After that, ammonia was added slowly to the solution and kept under continuous stirring for 20 min. After completion of the reaction time, the solution was

cooled for 20 min and it was preserved for gelation. The sol was allowed to age up to three weeks in a polypropylene container to be converted into gel.

Drying and calcination

After the aging process, the containers were partially opened for the solvent to evaporate very slowly and for the gel to dry up to a constant weight. The above process was carried out at room temperature. The dried gel was calcined at 1000 °C, 1200 °C, and 1400 °C. Fig. 1 shows the flow sheet for the preparation of mullite gel. Fig. 2(a) shows the precursor sol and Fig. 2(b) shows the mullite gel formed.

Preparation of gel bonded castables

Materials

The starting raw materials of the castables are different grades of bauxite, calcined alumina, reactive alumina, and tabular alumina with 0.1% and 0.3% of MgO as additives [12, 19, 20]. Table 1 shows the batch composition of the prepared raw materials.

Two batches are prepared with different binder compositions—2%, 5%, 7%, and 10% of mullite gel was added with batch composition. Trial samples with B1 batch mullite gel resulted in powder. Trial sample with B4 batch mullite gel was highly flowable. Trial samples of B2 batch (5%) and B3 batch (7%) of mullite gel were taken for further studies.

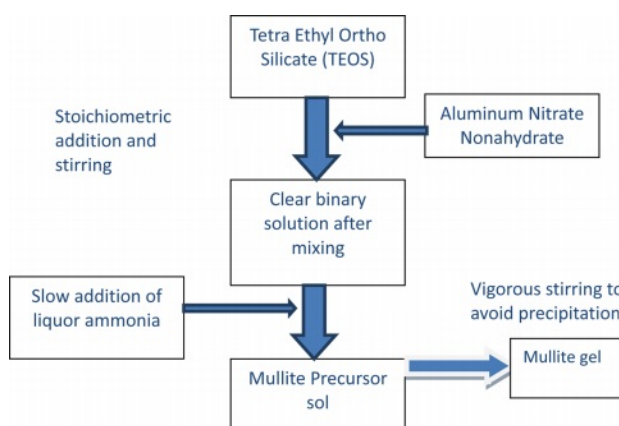


Fig. 1. Flow sheet for mullite sol preparation.

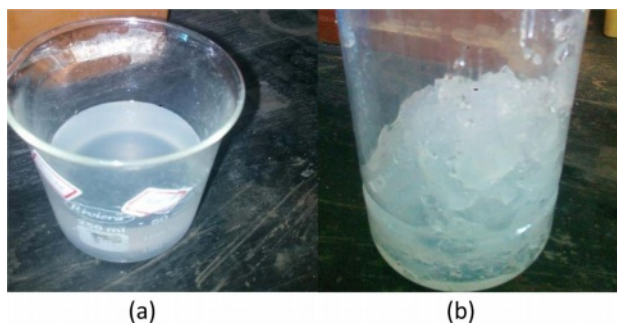


Fig. 2. (a) Stable sol precursor and (b) formation of gel.

Table 1. Batch composition

Raw materials	Batch A (0.1 wt % MgO binder)				Batch B (0.3 wt %MgO binder)			
	B1	B2	B3	B4	B1	B2	B3	B4
Bauxite (5/10)	15	15	15	15	15	15	15	15
Bauxite (3/5)	15	15	15	15	15	15	15	15
Bauxite (1/16)	20	20	20	20	20	20	20	20
Calcined alumina (-325)	10	10	10	10	10	10	10	10
Reactive alumina (-325)	10	10	10	10	10	10	10	10
Tabular alumina (-325)	10	10	10	10	10	10	10	10
Water	10	10	10	10	10	10	10	10
Mullite gel	2%	5%	7%	10%	2%	5%	7%	10%

Castable preparation

The castables were prepared by using the wet process method. The raw materials were dried and mixed with different percentages of mullite gel (say 1 mL of gel in 100 g of batch) [21]. In order to obtain the desired flow and consistency of the mixer solution, the required amount of water was added. The mixed composition was cast in steel molds of the following dimensions: 50 mm cube and 120 mm × 40 mm × 40 mm rectangular bar shapes. It was allowed for 24 h curing in the mold. The cast shapes were demolded and cured in air for 24 h and then oven-dried at 110 °C. Fig. 3 shows the developed mullite bonded castables. After drying, it was heat-treated at 1100 °C and 1300 °C for property evaluation.

**Fig. 3.** Gel bonded castable brick.

Characterization Studies

Characterization of mullite gel

Solid content

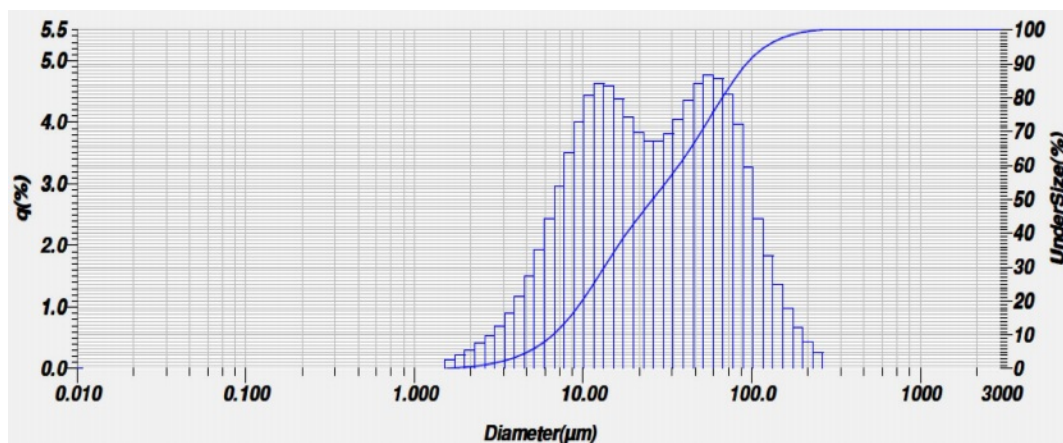
The solid content for the dried mullite gel was determined by using the ignition method at 1000 °C and was found to be around 25%.

Particle size analysis

The particle size distribution plot is shown in Fig. 4. All the dried gel particles are calcined at 1000 °C and found to be in the size range of 3-100 μm with an average particle size around 10 μm. The particle of the D_{50} range is 340.7 μm.

DSC-TG

Fig. 5 shows the DSC-TG curve of the mullite precursor gel. There is a gradual weight loss from 250 °C to 1200 °C. Fig. 5 shows the two exothermic peaks at 45 °C and 129 °C which also indicate that the mullite gel exhibits a strong exothermic peak which corresponds to the evaporation of organic materials in the gel. The peak at 610 °C corresponds to the formation of mullite phase. The phase formation starts in the temperature range of 330 °C to 820 °C. Around 800 °C the weight loss of mullite gel due to the evaporation of water and

**Fig. 4.** Particle size distribution of mullite sol.

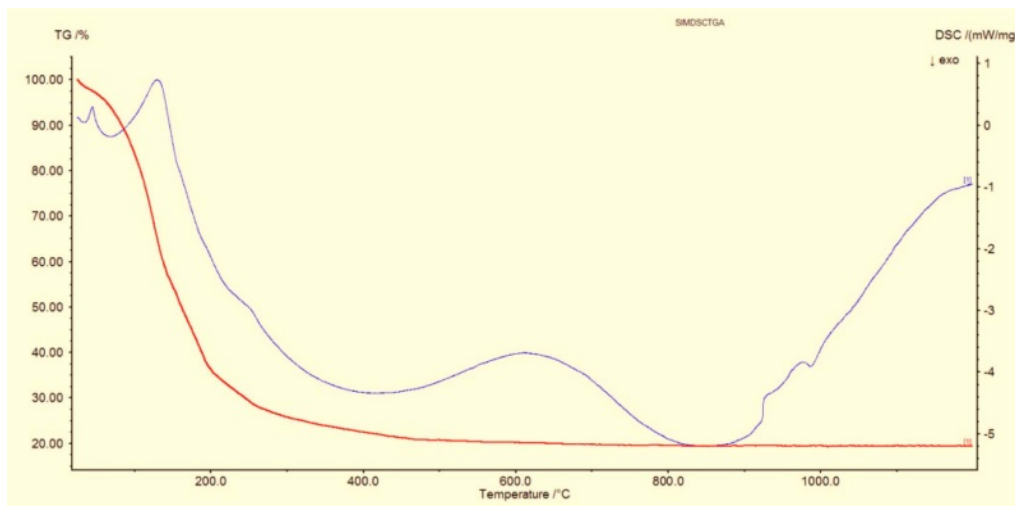


Fig. 5. DSC-TG pattern of mullite gel.

volatile materials followed by the decomposition of organic materials and nitrates can be observed. The small endothermic peak at 995 °C denotes the evaporation of nitrates and alumina materials and it slowly forms the mullite crystallization. The complete mullite curve reaches the temperature levels of 1100 °C–1200 °C during this analysis.

XRD

X-ray diffraction analysis was carried out for the powdered samples calcined at different temperatures. Fig. 6 shows the XRD patterns of the mullite gel calcined at 1000 °C, 1200 °C, and 1400 °C. This result indicates the formation of pure mullite crystals (JCPDS No.15-0776) at the calcination temperature of 1400 °C in the alumina along with traces of mullite [22]. And the Si replacement in alumina takes place leading to the formation of mullite as detected in the powders [23].

Fig. 6 shows that at the calcination temperatures of 1000 °C and 1200 °C, there is no phase formation and are found to appear as an amorphous phase. At 1400 °C, formation of mullite phase can be observed along with minor amounts of amorphous phases.

Microstructural analysis

The microstructure of mullite powders calcined at 1400 °C is shown in Fig. 7. The SEM micrograph in Fig. 7(a) shows small distributed and little agglomerated spherical particles in the size range between 46.3 nm and 65.5 nm with the maximum value of spherical particles being around 118.8 nm. EDX analysis as shown in Fig. 7(b) confirms the presence of aluminum, silica, and oxygen.

Characterization of castables

XRD

Fig. 8 shows the XRD pattern of the castables. It

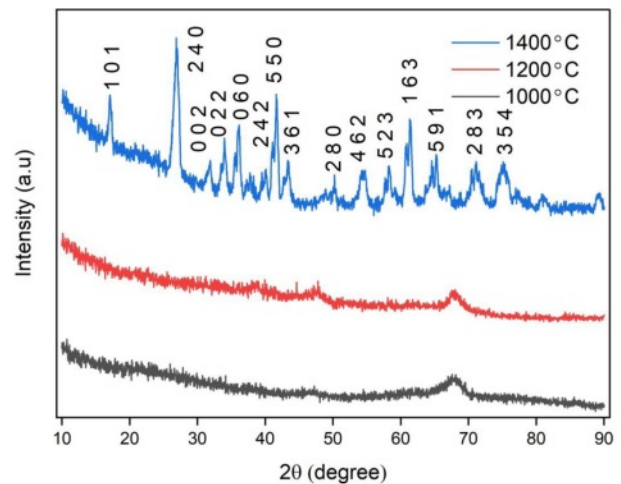


Fig. 6. X-ray spectra of mullite gel calcined at 1000 °C, 1200 °C and 1400 °C.

shows the presence of sharp crystalline peaks of alumina and mullite. The present XRD peaks were well matched with the JCPDS no. 06-0258 and also matched with the recent work done on mullite bonded castables [9]. No other impurity phases and unreacted phases were present in the sample.

Bulk density

The bulk density of the castables was measured as per American Society for Testing and Materials (ASTM). Fig. 9 shows the bulk density of the samples calcined at 1100 °C and 1300 °C for various percentages of gel added. The bulk density of the developed castables was found to increase with calcination temperature as shown in Fig. 9. Addition of mullite gel increases the density of the prepared castables due to the formation of mullite. The bulk density of the castables varied from 2.67–2.7 g/cc.

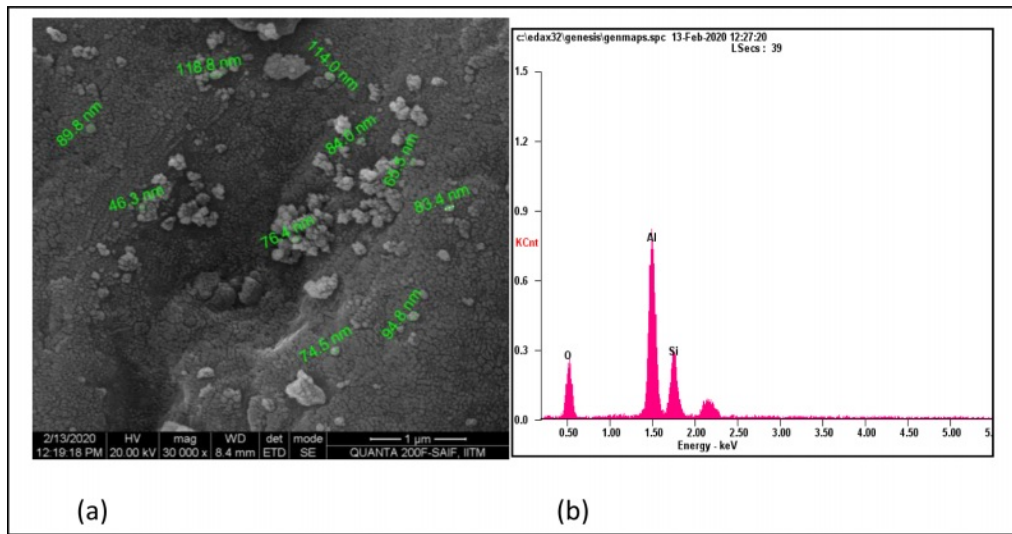


Fig. 7. (a) Microstructure of powders calcined at 1400 °C and (b) elemental analysis of powders calcined at 1400 °C.

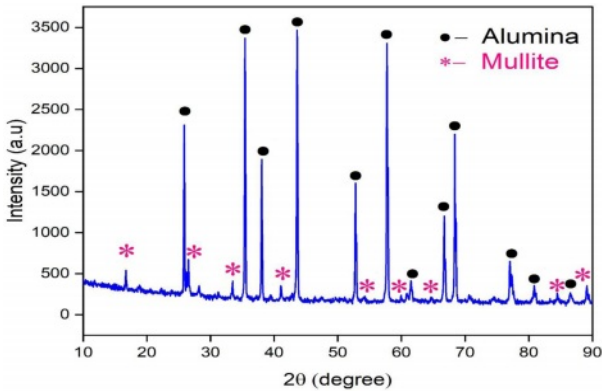


Fig. 8. XRD pattern of developed castables at 1300 °C.

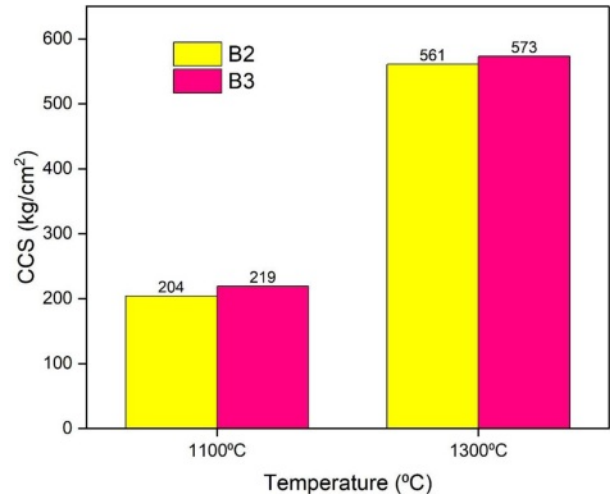


Fig. 10. Cold Crushing Strength of the developed castables.

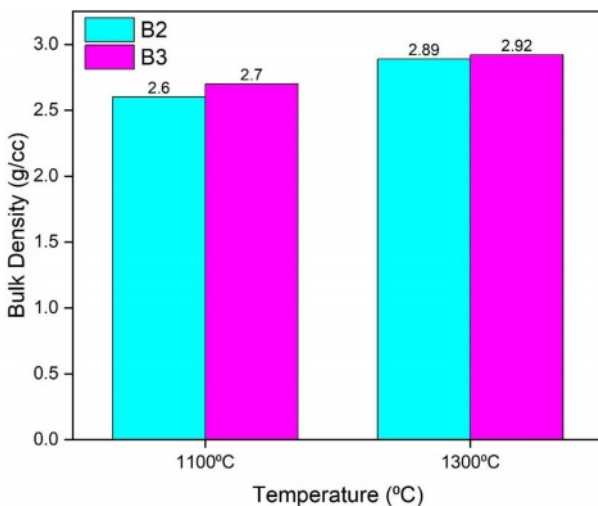


Fig. 9. Bulk density of developed castables.

Cold Crushing Strength

The Cold Crushing Strength (CCS) values of the different castable compositions at different processing

temperatures are shown in Fig. 10. It shows lower strengths under dried conditions due to the formation of mullite gel bonded castables; however, this increases the strength of the castables. The batch with 7% mullite gel resulted in higher CCS values compared to the batches containing 5% gel. The batches only measured the temperature levels at 1100 °C and 1300 °C. The formation of mullite leads to greater density and hence higher CCS values.

Modulus of rupture

The modulus of rupture of the developed castables is shown in Fig. 11. The initial cold modulus of rupture (CMOR) value of the dried samples was less due to weak bonding between the particles. Increase in temperature resulted in an increase in the CMOR values at 1300 °C. The batch with 7% mullite gel resulted in higher values of CMOR than 5% mullite gel.

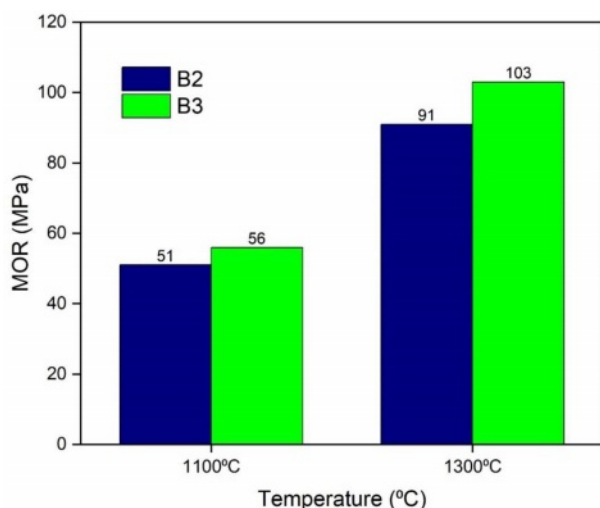


Fig. 11. MOR of developed castables.

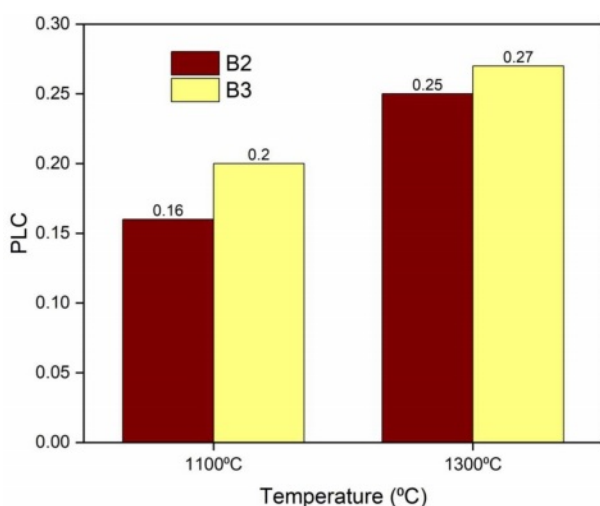


Fig. 12. PLC of developed castables.

PLC

The PLC of the castables is reported in Fig. 12. It was found to decrease the measured values. The PLC values after calcining at 1100 °C and 1300 °C are slightly increased. The increase in PLC is caused due to the volumetric expansion of mullite in the castables. An increase in temperature resulted in an increase in the PLC value.

Conclusion

The pure mullite gel bonded alumina castables were obtained in various compositions and the various physical and thermal properties were studied. The quality properties of mullite gel bonded alumina castables were obtained. The developed mullite gel bonded alumina castables showed improved physical and mechanical properties when compared to the commercial alumina castables. The presence of mullite along with the addition of 0.1 wt% and 0.3 wt% MgO resulted in a

significant improvement in the density and strength of the alumina castables at the temperature of 1300 °C. The presence of ultrafine mullite precursor particles led to improved sintering properties while using the conventional technique of processing. The prepared castables exhibited greater sintering properties with improved density and strength at 1300 °C which is higher than many conventional castables. These castables were modified to use in high temperature applications such as blast furnaces and steel ladles.

References

1. W.E. Lee, W. Vieira, S. Zhang, K. Ghanbari Ahari, H. Sarpoolaky, and C. Parr, *Int. Mater. Rev.* 46[3] (2001) 145-167.
2. V.K. Singh, M.M. Au, and U.K. Mandal, *Trans. Indian Ceram. Soc.* 52[4] (1993) 146-149.
3. A.K. Singh and R. Sarkar, *Int. J. Appl. Ceram. Technol.* 12 (2015) E54-E60.
4. C. Parr, H. Fryda, and C. Wöhrmeyer, *J. South. African Inst. Min. Metall.* 113[8] (2013) 619-629.
5. J. Xiong, Y. Peng, D. Xie, and X. Mao, *Adv. Mater. Res.* 396-398 (2012) 288-291.
6. S. Mavahebi, M. Bavand-vandchali, and A. Nemati, *Ceram. Int.* 45[13] (2019) 16338-16346.
7. D. Ding, S. Yang, G. Xiao, Y. Ren, L. Lv, P. Yang, X. Hou, and J. Gao, *Int. J. Appl. Ceram. Technol.* 16[4] (2019) 1416-1424.
8. A.P. Luz, L.B. Consoni, C. Pagliosa, C.G. Aneziris, and V.C. Pandolfelli, *Ceram. Int.* 44[9] (2018) 10486-10497.
9. A.K. Singh and R. Sarkar, *Ceram. Int.* 42[11] (2016) 12937-12945.
10. H. Yaghoubi, H. Sarpoolaky, F. Golestanifard, and A. Souri, *Iran. J. Mater. Sci. Eng.* 9[2] (2012) 50-58.
11. M. Nouri-Khezrabad, M.A.L. Braulio, V.C. Pandolfelli, F. Golestani-Fard, and H.R. Rezaie, *Ceram. Int.* 39[4] (2013) 3479-3497.
12. B. Mandal, R. Sarkar, and P.K. Dasgopdar, *Ind. Ceram.* 31[3] (2011) 217-222.
13. R. Sarkar, *InterCeram Int. Ceram. Rev.* 69[4-5] (2020) 44-53.
14. A.K. Singh and R. Sarkar, *Trans. Indian Ceram. Soc.* 74[4] (2015) 225-231.
15. S. Ghosh, R. Majumdar, B.K. Sinhamahapatra, R.N. Nandy, M. Mukherjee, and S. Mukhopadhyay, *Ceram. Int.* 29[6] (2003) 671-677.
16. S. Mukhopadhyay, S. Ghosh, M.K. Mahapatra, R. Mazumder, P. Barick, S. Gupta, and S. Chakraborty, *Ceram. Int.* 28[7] (2002) 719-729.
17. L.S. Cividanes, T.M.B. Campos, L.A. Rodrigues, D.D. Brunelli, and G.P. Thim, *J. Sol-Gel Sci. Technol.* 55[1] (2010) 111-125.
18. H. Tan, *J. Ceram. Process. Re.* 13[5] (2012) 575-578.
19. L.A. Díaz, R. Torrecillas, A.H. de Aza, and P. Pena, *J. Eur. Ceram. Soc.* 27[16] (2007) 4623-4631.
20. V.S. Pinto, D.S. Fini, V.C. Miguel, V.C. Pandolfelli, M.H. Moreira, T. Venâncio, and A.P. Luz, *Ceram. Int.* 46[8] (2020) 11137-11148.
21. A.P. Luz, S.J.S. Lopes, D.T. Gomes, and V.C. Pandolfelli, *Ceram. Int.* 44[8] (2018) 9159-9167.
22. X.H. Jin, L. Gao, and J.K. Guo, *J. Eur. Ceram. Soc.* 22[8] (2002) 1307-1311.
23. J.E. Lee, J.W. Kim, Y.G. Jung, C.Y. Jo, and U. Paik, *Ceram. Int.* 28[8] (2002) 935-940.